Effects of low Ag additions on the hydrogen permeability of Pd–Cu–Ag hydrogen separation membranes

Nayebossadri, Shahrouz; Speight, John; Book, David

DOI:
10.1016/j.memsci.2013.10.002

Journal of Membrane Science 451 (2014) 216–225

Contents lists available at ScienceDirect

Journal of Membrane Science

journal homepage: www.elsevier.com/locate/memsci

Effects of low Ag additions on the hydrogen permeability of Pd–Cu–Ag hydrogen separation membranes

Shahrouz Nayebossadri *, John Speight, David Book

School of Metallurgy and Materials, University of Birmingham, Edgbaston, Birmingham B15 2TT, UK

ARTICLE INFO

Article history:
Received 21 June 2013
Received in revised form
24 September 2013
Accepted 1 October 2013
Available online 8 October 2013

Keywords:
Hydrogen separation
Metallic membrane
Palladium-based ternary alloys
Pd–Cu
Pd–Cu–Ag

ABSTRACT

Pd–Cu alloys are of potential interest for use as hydrogen purification membranes, but have relatively low permeability compared to the commercially used alloys such as Pd–Ag. In this work, the effects of partial Ag substitution on the hydrogen diffusivity, solubility and the permeability of Pd–Cu membranes with a bcc structure have been investigated. With the addition of 2.3 and 3.9 at% Ag to Pd–Cu, lattice expansions of 0.11% and 0.35% were observed. Structural analyses by *in-situ* XRD showed that the bcc structure of the 2.3 at% Ag alloy is retained upon heating to 600 °C, whereas an fcc phase forms in the 3.9 at% Ag alloy resulting in a mixed (bcc+fcc) structure. Whilst the diffusion coefficients between 350 and 400 °C for both Pd–Cu–Ag ternary samples were shown to be lower than their binary alloys (which had similar structures), higher solubility values were obtained. The lower diffusion coefficients of the ternary alloys are related to an increase in the diffusion activation barrier in the presence of Ag, and the higher solubility values may be attributed to the lattice expansion and high Ag–H chemical interaction. Hydrogen permeation measurements showed that an enhancement in the hydrogen solubility of the bcc phase $Pd_{45.8}Cu_{51.9}Ag_{2.3}$, does not have a substantial effect on the permeability of the membrane. In contrast, for the $Pd_{45.1}Cu_{51}Ag_{3.9}$ sample with a mixed (bcc+fcc) phase, higher hydrogen solubility can lead to a remarkable improvement in permeability. Hence, it is suggested that the hydrogen permeability in the bcc phase is mainly controlled by hydrogen diffusion, and the solubility enhancement can only significantly improve the hydrogen permeability when the fcc phase is present.

1. Introduction

The commercial hydrogen separation by metallic membranes is mainly focused on palladium alloys. The interest in Pd is due to the high hydrogen transport ability over a wide temperature range as a result of a higher solubility and diffusivity of the face centred cubic (fcc) form of this metal comparing to the other elements in group 10. However, the practical application of pure Pd membranes is limited due to the Pd–Hydrogen system exhibiting two distinct immiscible α (interstitial hydrogen solid solution, $T < 298$ °C) and β (palladium hydride) phases. Transition between the α and β phases is accompanied by a volume increase of 10%, which results in lattice distortion, the formation of high internal stresses, deformation, and ultimately failure of the membrane [1,2]. This problem, in conjunction with susceptibility of the pure Pd to surface poisoning by impurity gases [3,4] and the high cost of Pd have led to the exploration of a wide variety of Pd-alloy membranes, such as Pd–Ag, Pd–Cu, and Pd–Y [5–10].

Amongst these alloys, palladium–copper (Pd–Cu thereafter) is of particular interest and has been extensively studied [11–18]. It was shown [11] that the permeability of Pd–Cu alloys is greatly influenced by the Cu content and hence, crystal structure of the alloy (Fig. 1). An extensive phase diagram study detailing the various phases present in the Pd–Cu alloy, was performed by Subramanian and Laughlin [19]. Consequently phase equilibria and thermodynamic properties on the Pd–Cu system were optimised using the CALculation of PHAse Diagram (CLAPHAD) technique [20,21]. However, the previous work in this lab [22] seems to be in a good agreement with the phase diagram proposed by Subramanian and Laughlin [19]. The phase diagram of Pd–Cu [19] shows terminal solid solutions based on Pd and Cu. An ordered structure of Cu_3Pd forms with $AuCu_3$-type structure over the entire composition range 10–20 at% Pd. This phase transforms to an ordered tetragonal structure (Cu_3Pd-type) with the Pd concentration ranging from 19 to 27 at%. In addition, ordered bcc solid solution of CuPd (β phase: CsCl-type) exists approximately from 35 to 50 at% Pd. A mixed phase region of body centred cubic (bcc) and face centred cubic (fcc, α phase), lies adjacent to the either side of the β phase. Also, increase in copper up to approximately 33 at%, in the terminal fcc Pd solid solution leads to a gradual reduction in the hydrogen permeability [11]. In contrast, higher hydrogen

* Corresponding author. Tel.: +44 121 414 5213.
E-mail address: s.nayebossadri@bham.ac.uk (S. Nayebossadri).

0376-7388/$ - see front matter © 2013 Elsevier B.V. All rights reserved.
http://dx.doi.org/10.1016/j.memsci.2013.10.002

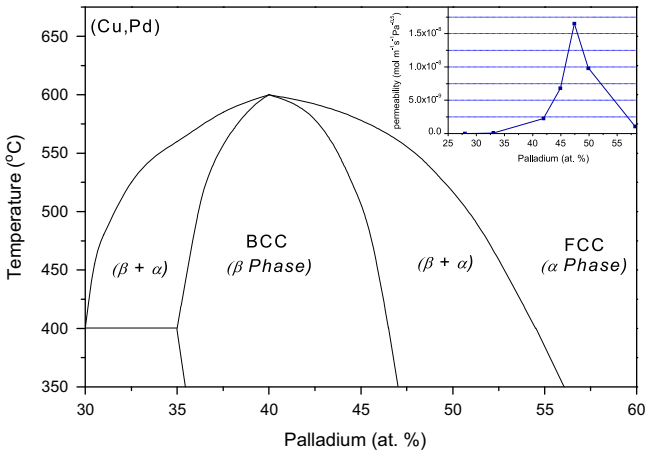

Fig. 1. High temperatures Pd–Cu phase diagram. Phase boundaries reproduced from Subramanian and Laughlin [19]. The inset graph shows variation in the hydrogen permeability versus palladium content at 350 °C, taken from Ref. [11].

permeability than that of pure Pd was reported [11] for the $Pd_{47}Cu_{53}$ (at%) alloy at 350 °C, which has a CsCl-type ordered bcc structure [19]. The remarkable enhancement in the hydrogen permeability of the bcc Pd–Cu alloy was attributed to the structural transition from fcc to bcc. Hydrogen diffusion is two orders of magnitude higher in the ordered bcc phase compared to the fcc phase, at ambient temperature [11–13,17].

A major limitation of Pd alloy membranes is susceptibility to poisoning by trace impurities in the gas stream, notably of CO and S species [23]. The effect has been shown to be crystal structure sensitive. It was reported that hydrogen flux through the bcc phase is undetectable only after 5 min exposure of the $Pd_{47}Cu_{53}$ (at%) membrane to 1000 ppm H_2S [24]. In contrast, Pd–Cu alloy membranes with fcc structure, have been reported to have high resistance to surface poisoning by H_2S [25–27]. It has been suggested that this resistance to S containing species results from the specific surface chemistry of the fcc phase [4,25], which is predominantly controlled by electronic factors [4,27]. As a result, efforts were made to improve the hydrogen flux through a range of Pd–Cu membranes with fcc structure [28–30]. Ideally, any modification induced by alloying should have a minimal effect on the surface and electronic properties of the Pd–Cu membrane in order to maintain the desired resistance to surface poisoning.

The potential of ternary metal alloys consisting of Pd, Cu and a third metallic element for hydrogen purification has been investigated by first principle calculations [31]. It was shown that higher hydrogen permeability can be achieved by selected metallic alloys addition to Pd–Cu but the effects of these additives on the hydrogen solubility and the diffusivity may be opposed. In an extension of this work, it was suggested that substituting a small amount of Cu with Ag in a binary fcc Pd–Cu alloy can improve both hydrogen solubility and diffusivity. However, if Pd is partially replaced by Ag in a binary Pd–Cu alloy, hydrogen solubility decreases and diffusivity increases [32]. Hence, it was concluded that permeability can be increased if only a small amount of Cu is substituted by Ag. More recently, hydrogen solubility, diffusivity, and permeability were predicted using Density Functional Theory (DFT) for calculating a range of the Pd–Cu–Ag ternary alloys with fcc structure [33]. It was concluded that substituting Ag for Pd or Cu can increase the hydrogen permeability and that enhancement is more closely related to increased hydrogen solubility rather than diffusivity [33].

In addition, the permeability of Pd–Cu–Ag ternary films deposited on porous stainless steel substrate by electroless plating was shown to be almost twice the permeability of thin film binary Pd–Cu alloys with similar compositions [28]. The effects of various Ag concentrations on the permeability of the Pd–Cu–Ag films fabricated by magnetron sputtering system were also examined between 300 and 400 °C. It was observed that replacement of Cu by only 1 at% of Ag can decrease the activation energy for hydrogen permeation by approximately 17% and enhance the permeability in the fcc phase by almost 50% in comparison to the counterpart binary alloy. Further replacement of Pd and Cu with Ag up to approximately 14 at% offered higher permeability than corresponding binary alloys, but had a less significant effect on the permeability than the addition of 1 at% Ag [30]. Subsequently, Ag and Cu segregation in the Pd–Cu–Ag films with fcc structure fabricated by sequential electroless plating method was investigated and showed that Cu and Ag segregations occur after annealing up to 500 °C for 5 days, even at low Ag concentrations of 4 and 7 at% [29].

The general trend suggested by previous work is that replacing Pd and Cu with a small amount of Ag can significantly improve the hydrogen permeability of fcc Pd–Cu membranes. Nevertheless, effects of Ag on the solubility, and particularly diffusivity of the Pd–Cu–Ag alloys in the bcc phase require further investigation. In this work, the effects of low Ag concentrations on the solubility, diffusivity, and finally permeability of the Pd–Cu–Ag alloys having bcc and mixed (bcc+fcc) structures are investigated. For comparison, solubility, diffusivity, and permeability of binary Pd–Cu alloys with bcc and mixed (bcc+fcc) structures are also investigated. Possible effects of Ag on the solubility, diffusion, and the permeability of each alloy are discussed.

2. Materials and method

Binary and ternary alloys with the nominal atomic compositions of $Pd_{47}Cu_{53}$ (sample 1), $Pd_{50}Cu_{50}$ (sample 2), $Pd_{46}Cu_{51}Ag_3$ (sample 3), and $Pd_{45}Cu_{50}Ag_5$ (sample 4) were supplied by Johnson Matthey Noble Metals (Royston, UK). Typically, in the as-received state the alloys had been cold-rolled from cast ingots into foils with varying thicknesses between 30 and 100 μm. X-Ray Diffraction (XRD) measurements of the foil were obtained by a Bruker D8-Advanced diffractometer using monochromatic CuKα radiation ($\lambda = 1.54056$ Å). Lattice spacing derived from the XRD patterns were used to determine the structure and Pd composition of the membranes. An Anton Parr XRK900 high-temperature sample cell was used to measure the temperature dependence of ternary alloy crystal structure under 100 kPa flowing He (100 ml/min) and heated at 2 °C min^{-1}. Thickness measurements of the foils and further compositional analyses on the cross section of the samples were performed using a Joel 6060 Scanning Electron Microscopy (SEM) equipped with an INCA 300 Energy Dispersive Spectroscopy (EDS).

Hydrogen flux was measured using a hydrogen permeation system designed and built in the School of Metallurgy and Materials [34]. Membrane disks with an area of 2.54 cm^2 were stamped from the rolled foils, washed in acetone and placed between an annealed copper gasket and a knife-edge to give a leak-free seal. A leak test was performed applying a pressure differential of 345 kPa using nitrogen gas (99.95%), supplied by BOC. The system was de-gassed under 10^{-6} kPa vacuum prior to hydrogen (99.99995%, BOC) admittance. The feed gas was controlled using Brookes 5850S Mass Flow Controller (MFC) calibrated over a range of 6–600 ml min^{-1} with an accuracy of ± 6 ml min^{-1}. A constant upstream pressure of 445 kPa was applied by continuous hydrogen flow and bled using another Brookes 5850S MFC. Downstream pressure was maintained at 100 kPa at all times using a back-pressure regulator. The permeated gas flow was measured by Brookes 5850S MFC placed after the back-pressure regulator. The temperature of both the membrane and the

upstream atmosphere was increased to over 400 °C using an Elite Thermal Systems Ltd. split furnace with a ramp-rate 2 °C min^{-1}.

Gravimetric hydrogen solubility measurements were performed using a constant-pressure TGA (Hiden Isochema Intelligent Gravimetric Analyser, IGA). The surface of the foils were lightly abraded, cleaned in acetone and dried before loading into the IGA. The samples with a weight of approximately 130 mg were loaded, activated in 2000 kPa hydrogen until saturated, then heated to 400 °C and thoroughly de-gassed under 10^{-7} kPa vacuum prior to cooling. Samples were then subjected to the various hydrogen pressures (100–500 kPa) and the weight changes were recorded at 350, 375 and 400 °C. Hydrogen concentration, C_H, was calculated based on the recorded weight change and the hydrogen solubility constant, K_S, of each alloy for dilute H concentration was calculated from the slope of the line according to Sievert's law ($c_H = K_S P_{H_2}^{1/2}$). Diffusion coefficients were calculated using Fick's first law according to the following equation [35]:

$$J = DA\Delta c/x \quad (1)$$

where J is the hydrogen flux, D is the diffusion constant, A is the surface area of membrane, Δc is the difference between upstream and downstream and x is the membrane thickness.

3. Results

3.1. Structural and compositional characterisation

The XRD patterns of the as-received (As-R) and the annealed binary and ternary alloys are shown in Fig. 2(a–h). The samples are numbered from 1 to 4, as noted earlier. All samples show relatively narrow peaks corresponding to the fcc structure in the As-R state due to the quenching from the single fcc region of the Pd–Cu phase diagram (Fig. 2a–d). As a result of cold rolling, a preferential orientation along the (220) plane is observed for all samples except one of the binary Pd–Cu alloys, sample 2, which shows a high intensity peak along the (111) plane. The XRD patterns of the samples after annealing for 72 h at 400 °C under vacuum are shown in Fig. 2 (e–h). Whilst, a fully bcc structure can be observed for both annealed samples (1) and (3) in Fig. 2e and f, the XRD patterns after annealing samples (2) and (4) show a mixed (bcc+fcc) structure (Fig. 2g and h). The Pd atomic composition x_{Pd} for binary Pd–Cu alloys can be calculated from fcc lattice constant a, versus composition for Pd–Cu, using the following equation derived by a linear fit of literature lattice parameters [14,15]:

$$a_{fcc} = 0.36462 + (2.44 \times 10^{-4})x_{Pd} \quad (2)$$

Using the same method, concentrations of Pd in ternary Pd–Cu–Ag alloys were estimated assuming that a low Ag concentration does not modify lattice parameter considerably. In fact, a difference of about 0.12% in the lattice parameter of the $Pd_{68}Cu_{25}Ag_7$ and the respecting Pd–Cu alloy was reported, which corresponds to less than 3% variation in the Pd composition [28,29]. Here, Pd compositions are calculated by averaging the four most intense fcc peaks for the As-R samples. Also compositions were determined by EDS, averaging various area scans ($> 10^3$ μm^2) of cross section for As-R samples and the results are listed in Table 1. It is observed that the Pd content determined by XRD and EDS are almost identical in the case of binary alloys, samples (1) and (2). However, the Pd content determined by EDS for sample (4) is considerably lower than that calculated by XRD. It is worth mentioning that no significant variation in the composition was observed by EDS, scanning several areas of the cross section of sample (4). Lattice parameters as a function of Pd composition for previously reported binary Pd–Cu alloys are plotted in Fig. 3 [14,15,36–38]. Whilst the lattice expansion for sample (3) with a lower Ag content (2.3 at%) is about 0.11% in comparison to the binary alloy with the same palladium content, a more pronounced lattice expansion of over 0.35% is observed for sample (4) with a higher Ag content (3.9 at%). It seems that Eq. (2) overestimates Pd content of the sample (4), as it fails to exclude the effect of lattice expansion induced by the Ag addition. Overestimating the Pd content by Eq. (2) can be also seen in Table 1 in the case of sample (3) with lower Ag content, but the Pd concentration obtained from XRD seems to deviate more from the actual value as the Ag content increases. Hence, compositions obtained by EDS analyses are accepted and referred hereafter.

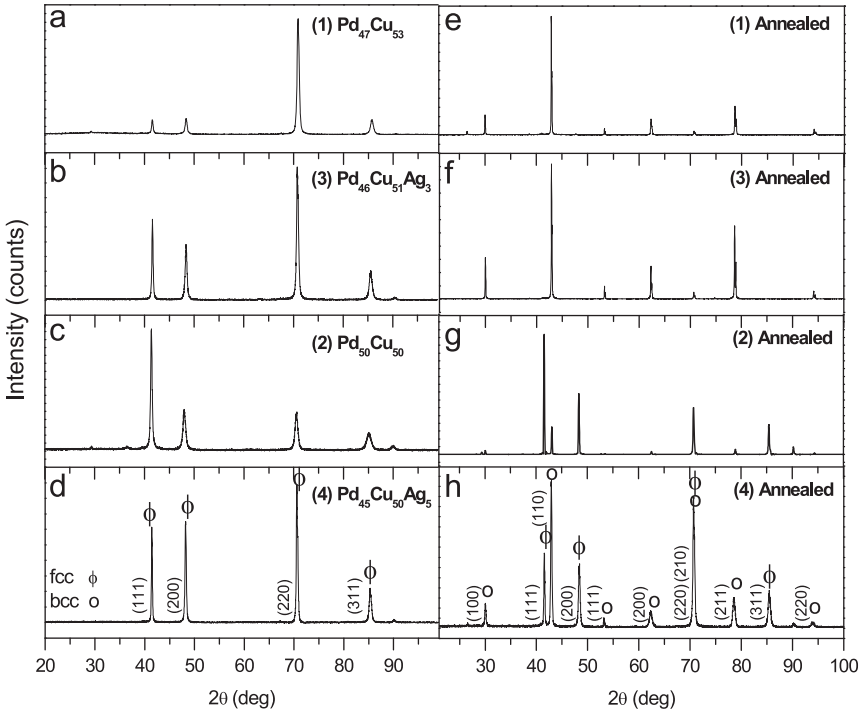

Fig. 2. XRD diffraction patterns of as received samples (a–d) and annealed (72 h at 400 °C under vacuum) samples (e–h).

Table 1
XRD and EDS analyses of the As-R binary Pd–Cu and ternary Pd–Cu–Ag alloys used in this study.

Samples	XRD (at%)		EDS (at%)		Lattice parameter a (nm)	Thickness (μm)	Comments
	Pd	Pd	Cu	Ag			
(1) Pd–Cu	46.5 ± 0.2	46.6 ± 0.4	53.4 ± 0.4	–	0.3759	40	bcc
(2) Pd–Cu	53.2 ± 0.5	53.1 ± 0.4	46.9 ± 0.4	–	0.3775	102	(bcc+fcc)
(3) Pd–Cu–Ag	47.4 ± 0.5	45.8 ± 0.4	51.9 ± 0.3	2.3 ± 0.2	0.3761	40	bcc
(4) Pd–Cu–Ag	51.5 ± 0.3	45.1 ± 0.5	51.0 ± 0.3	3.9 ± 0.2	0.3771	35	(bcc+fcc)

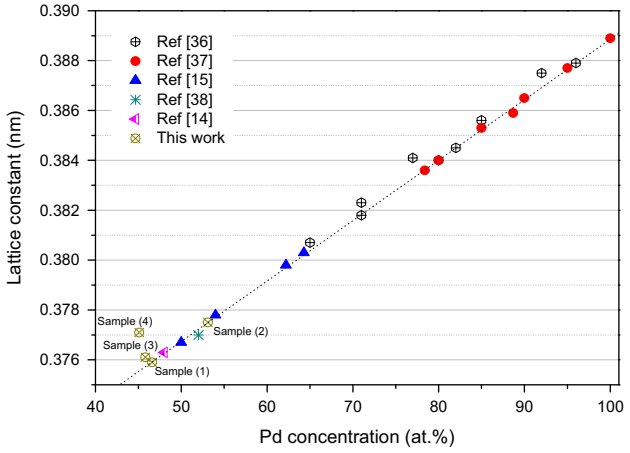

Fig. 3. Lattice constants of the fcc Pd–Cu alloys as a function of Pd concentration. The lattice constants of the binary $Pd_{46.6}Cu_{53.4}$ (sample 1) and $Pd_{53.1}Cu_{46.9}$ (sample 2) and the ternary $Pd_{45.8}Cu_{51.9}Ag_{2.3}$ (sample 3) and $Pd_{45.1}Cu_{51}Ag_{3.9}$ (sample 4) alloys used in this study are included for the comparison. Dotted line is a guide for the eye.

Furthermore, based on the binary Pd–Cu phase diagram [19] and the Pd content of sample (4), the existence of a mixed (bcc+fcc) phase after annealing (Fig. 2h) is unexpected as the Pd content is well located within the bcc phase. Also, co-existence of fcc and bcc phases is unlikely to be a kinetic issue with annealing condition used in the present work, because the fcc Pd–Cu to bcc transition is a disorder to order transition requires only local rearrangement of atoms and does not involve long range diffusion [14]. To further investigate this, the structures of both As-R ternary Pd–Cu–Ag alloys, samples (3) and (4), were monitored during heating and subsequent cooling by *in-situ* XRD. The heating and cooling cycle of sample (3) is shown in Fig. 4. It is evident that the initial fcc structure almost completely converts to a bcc structure above 350 °C, which remains present until the reappearance of the fcc phase above 550 °C. Upon cooling the sample from 600 °C, the bcc phase regains its intensity, whilst a small amount of fcc phase is still remaining, probably due to the insufficient time for phase transition. In contrast to sample (3), the evolution of phases in sample (4) with higher Ag content (3.9 at%) suggests that the phase transition during heating and cooling cycle may not be appropriately described by the binary phase diagram [19]. In the heating and cooling cycle of sample (4) (Fig. 5), a significant amount of the initial fcc structure of the sample is retained. Peaks with low intensities corresponding to the bcc phase are only observed after 350 °C. On cooling from 600 °C, the relative amount of the bcc phase gradually increases at lower temperatures ($T < 500$ °C). Therefore, it is suggested that Ag addition may contract the bcc Pd–Cu ordered phase region and promotes fcc phase formation at higher temperatures, even with such a low Ag content.

3.2. Diffusivity and solubility

Diffusivity and solubility values of samples (1) and (3) as a function of temperature (350–400 °C), with a bcc structure, are shown in Fig. 6a and b (diffusivity and solubility values of samples (1) and (3) are also included in Table 2). A diffusion coefficient of 2.8×10^{-4} cm^2 s^{-1} was obtained for sample (1) at 350 °C, which increased to 5.6×10^{-4} cm^2 s^{-1} at 400 °C (Fig. 6a). These results show a good agreement with the experimentally and computationally determined diffusion range of approximately 2–6.5×10^{-4} cm^2 s^{-1} for the same temperature range reported in the literature [12,17,39,40]. Lower diffusion coefficients are observed (Fig. 6a) for the $Pd_{45.8}Cu_{51.9}Ag_{2.3}$ ternary alloy, sample (3), between 350 and 400 °C in comparison to the binary $Pd_{46.6}Cu_{53.4}$ alloy, sample (1). It is also evident the difference between the diffusion coefficient of samples (1) and (3) is continuously increasing as the temperature increases. Ultimately this results in the diffusion coefficient value of sample (1) being almost 50% higher than sample (3) at 400 °C. In contrast, solubility constants at 350 °C of 9.3×10^{-6} and 9.7×10^{-6} Pa$^{-0.5}$ were obtained for samples (1) and (3), respectively (see Fig. 6b). Whilst the solubility constant of sample (3) is slightly higher than the solubility constant of sample (1) at 350 °C, the magnitude of difference in the solubility seems to increase at higher temperatures. Sample (3) represents a solubility constant which is almost 60% higher at 400 °C in comparison to the solubility constant of sample (1). Therefore, whilst the ternary alloy (sample 3) with a bcc structure has lower diffusion coefficients in comparison to the binary alloy with the same structure over the studied temperature range, the hydrogen solubility is remarkably improved for the ternary alloy containing a small amount of Ag.

Diffusivity and solubility values of samples (2) and (4) which had mixed (bcc+fcc) structure are shown in Fig. 6c and d (diffusivity and solubility values of samples (2) and (4) are also included in Table 2). Diffusion coefficient values of 2×10^{-4} and 1.7×10^{-4} cm^2 s^{-1} were found for samples (2) and (4) at 350 °C respectively in Fig. 6c, showing that the diffusion coefficient of the ternary alloy, sample (4), is approximately 15% lower than that of binary alloy, sample (2). This ratio seems to remain almost constant with the increasing of temperature to 400 °C. Surprisingly, once the temperature increases from 350 to 400 °C, diffusion coefficients for both samples are decreased. According to the binary Pd–Cu phase diagram [19] once the temperature of sample (2) is increased, the relative percentage of fcc phase should increase, while the relative percentage of bcc phase decreases. Furthermore, our *in-situ* XRD result for sample (4) (see Fig. 5) confirms that the amount of bcc phase decreases at higher temperatures. Therefore, it is suggested that the reduction in the diffusion coefficient of both samples (2) and (4) during the heating process can be related to the progressive formation of the fcc phase and the continuous reduction of the bcc phase. Diffusion coefficient values of 9×10^{-5} for sample (2) and 4.5×10^{-5} cm^2 s^{-1} for sample (4) were obtained at 400 °C, which are in a good agreement with the reported values for fcc Pd–Cu alloys [12,39]. Fig. 6d shows that the solubility constant of sample (2) is slightly lower than that of sample (4) at 350 °C. However, sample (2) gives a solubility constant of 2.6×10^{-5} Pa$^{-0.5}$ at 400 °C which is about half the solubility constant of sample (4). Also, an increase in the solubility constant for both samples is observed at higher temperatures, which should correspond to increasing amounts of

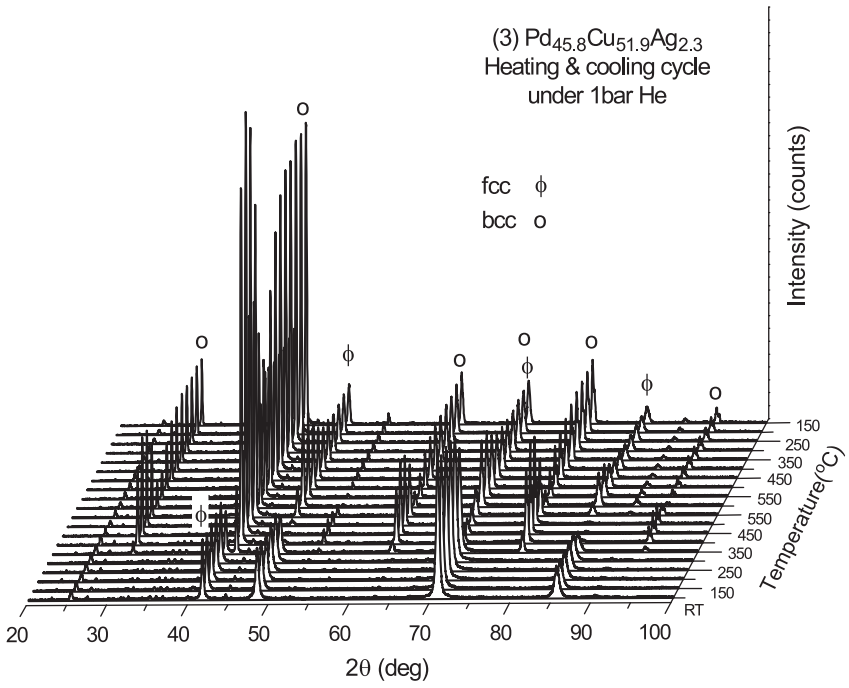

Fig. 4. Evolution of the *in-situ* XRD diffraction patterns for the $Pd_{45.8}Cu_{51.9}Ag_{2.3}$ (sample 3) as a function of temperature. The first XRD pattern was collected at room temperature (RT) and the subsequent patterns correspond to the 150–600–150 °C heating and cooling cycle under 100 kPa helium with 2 °C min^{-1} heating and cooling rate.

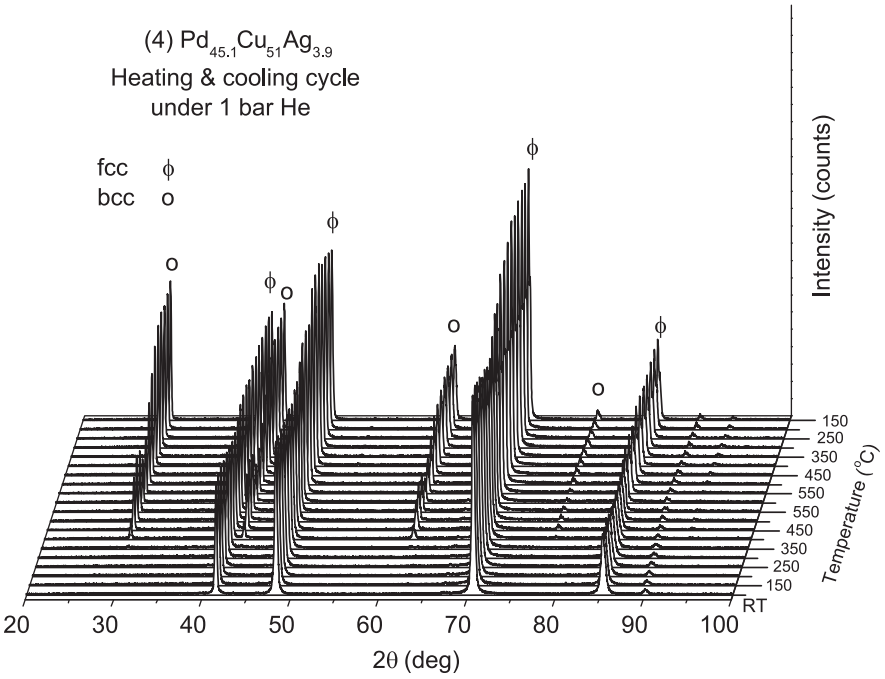

Fig. 5. Evolution of the *in-situ* XRD diffraction patterns for the $Pd_{45.1}Cu_{51}Ag_{3.9}$ (sample 4) as a function of temperature. The first XRD pattern was collected at room temperature (RT) and the subsequent patterns correspond to the 150–600–150 °C heating and cooling cycle under 100 kPa helium with 2 °C min^{-1} heating and cooling rate.

the fcc phase. In addition, the solubility constants observed here are generally higher than the solubility constant obtained for samples (1) and (3) with a bcc structure, which further confirms the marginal hydrogen solubility in the bcc structure [18]. As a result, whilst the diffusion coefficient of the ternary alloy (sample 4) with the mixed (bcc+fcc) structure is lower than that of binary alloys with the similar structure, a small amount of Ag seems to significantly improve the hydrogen solubility, especially once the amount of fcc phase increases.

3.3. Permeability

Hydrogen permeation through thick ($>10\,\mu m$) Pd and Pd-binary foils is commonly assumed to be limited by hydrogen diffusion through the bulk of the membrane as the rate of dissociation and recombination of hydrogen on the surface is much faster than the diffusion through the bulk of membrane [40,41]. To examine whether Ag addition can influence the rate of the surface reactions in the case of the ternary alloys used in this

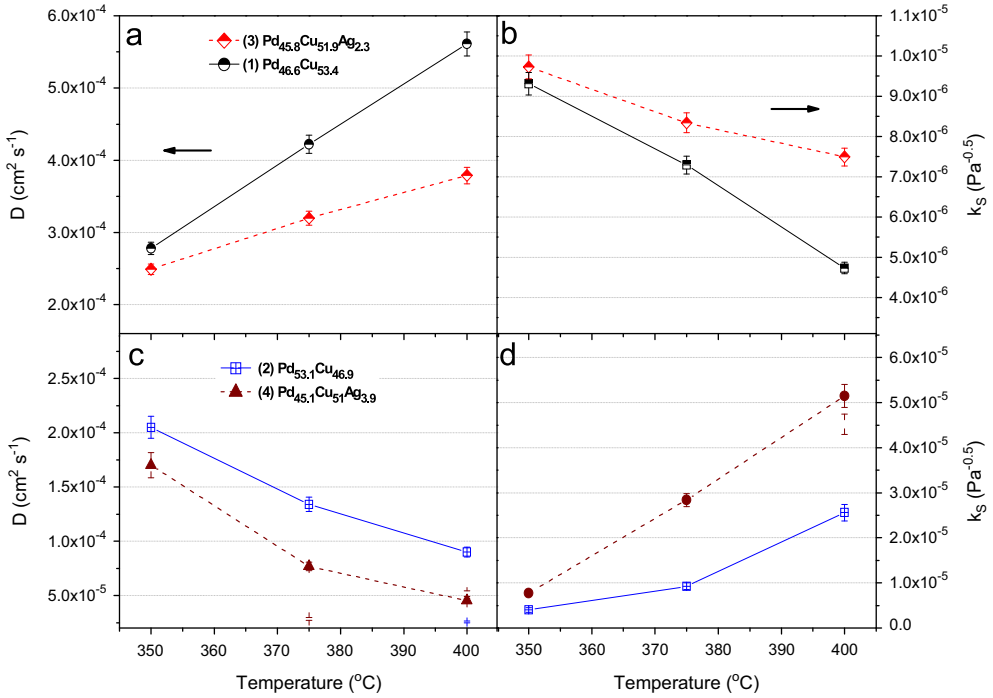

Fig. 6. (a) Hydrogen diffusion coefficients D, and (b) solubility constants K_S, for $Pd_{46.6}Cu_{53.4}$ (sample 1) and $Pd_{45.8}Cu_{51.9}Ag_{2.3}$ (sample 3) as a function of temperature. (c) Hydrogen diffusion coefficients D, and (d) solubility constants K_S, for $Pd_{53.1}Cu_{46.9}$ (sample 2) and $Pd_{45.1}Cu_{51}Ag_{3.9}$ (sample 4) as a function of temperature. Solid lines and dotted lines are guides for the eye.

Table 2
Calculated diffusivity and solubility values for binary Pd–Cu and ternary Pd–Cu–Ag alloys used in this study.

Sample	D ($cm^2\ s^{-1}$)			K_S ($Pa^{-0.5}$)		
	350 °C	375 °C	400 °C	350 °C	375 °C	400 °C
(1) $Pd_{46.6}Cu_{53.4}$	2.8×10^{-4}	4.2×10^{-4}	5.6×10^{-4}	9.3×10^{-6}	7.3×10^{-6}	4.7×10^{-6}
(2) $Pd_{53.1}Cu_{46.9}$	2×10^{-4}	1.3×10^{-4}	9×10^{-5}	4×10^{-6}	9.3×10^{-6}	2.6×10^{-5}
(3) $Pd_{45.8}Cu_{51.9}Ag_{2.3}$	2.5×10^{-4}	3.2×10^{-4}	3.8×10^{-4}	9.7×10^{-6}	8.3×10^{-6}	7.5×10^{-6}
(4) $Pd_{45.1}Cu_{51}Ag_{3.9}$	1.7×10^{-4}	7.7×10^{-5}	4.5×10^{-5}	7.7×10^{-6}	2.8×10^{-5}	5.15×10^{-5}

study, hydrogen permeation flux at several temperatures as a function of hydrogen differential pressures are plotted in Fig. 7. A good linear relationship is observed with pressure exponent equal to 0.5, which indicates that hydrogen concentration is proportional to the square root of hydrogen pressure and that shows the addition of Ag has no significant effect on the rate of hydrogen dissociation or recombination at the surface of the membrane. Assuming that the hydrogen diffusion is the rate determining step, the hydrogen permeability was determined by the following equation.

$$J = \emptyset \frac{P_1^n - P_2^n}{l} \tag{3}$$

where J is the hydrogen flux ($mol\ s^{-1}$), $\emptyset$ is the hydrogen permeability ($mol\ m^{-1}\ s^{-1}\ Pa^{-0.5}$), P_1 and P_2 are the hydrogen pressures (Pa) on the upstream and downstream side of the membrane respectively, n is the pressure exponent, which is 0.5 in the case of bulk diffusion, and l is the membrane thickness (m). Permeability values for all samples are shown in Fig. 8. In the present samples, hydrogen permeability becomes significant around 100 °C for all samples except sample (2), for which no hydrogen permeation is observed until over 200 °C. It should also be noted, the permeability values of Pd–Cu–Ag ternary alloys are lower than the permeability value of the $Pd_{46.6}Cu_{53.4}$ bcc binary alloy, sample (1), but higher than that of $Pd_{53.1}Cu_{46.9}$ binary alloy, sample (2), with a mixed (bcc+fcc) phase.

Fig. 9 compares the permeability of the Pd–Cu–Ag ternary alloys containing 2.3 and 3.9 at% Ag used in this study with each other and their corresponding binary alloys alongside pure Pd at 350 °C. Also, the permeability values for binary alloys, samples (1) and (2) are included for further comparison with the reported data in the literature [11]. However, it should be noted that a precise comparison is complicated due to the fact that permeability values are highly sensitive to the alloy composition and experimental conditions. In general, the permeability values obtained here for the binary alloys, samples (1) and (2) seem to be in a good agreement with the previously observed trend for binary Pd–Cu alloys shown in Fig. 9. The observed permeability values for the ternary alloys, samples (3) and (4) are also very similar to their respecting binary alloys. It has been suggested that diffusion coefficients for bcc Pd–Cu alloys are significantly larger than fcc Pd–Cu alloys and are relatively insensitive to the alloy composition [12,26]. In addition, the high hydrogen permeability of the Pd–Cu bcc phase is known to be a characteristic of the CsCl-type ordered structure of the Pd–Cu alloy [11]. In Fig. 6a and b, it was shown that whilst in the temperature range studied here the diffusion coefficients of sample (3) are lower than sample (1), it has higher solubility constants. However, the observed lower permeability of sample (3) in comparison with sample (1) further confirms that hydrogen permeability in the bcc phase is mainly dominated by diffusion. An improvement in the hydrogen solubility alone, cannot lead to the improved hydrogen permeability.

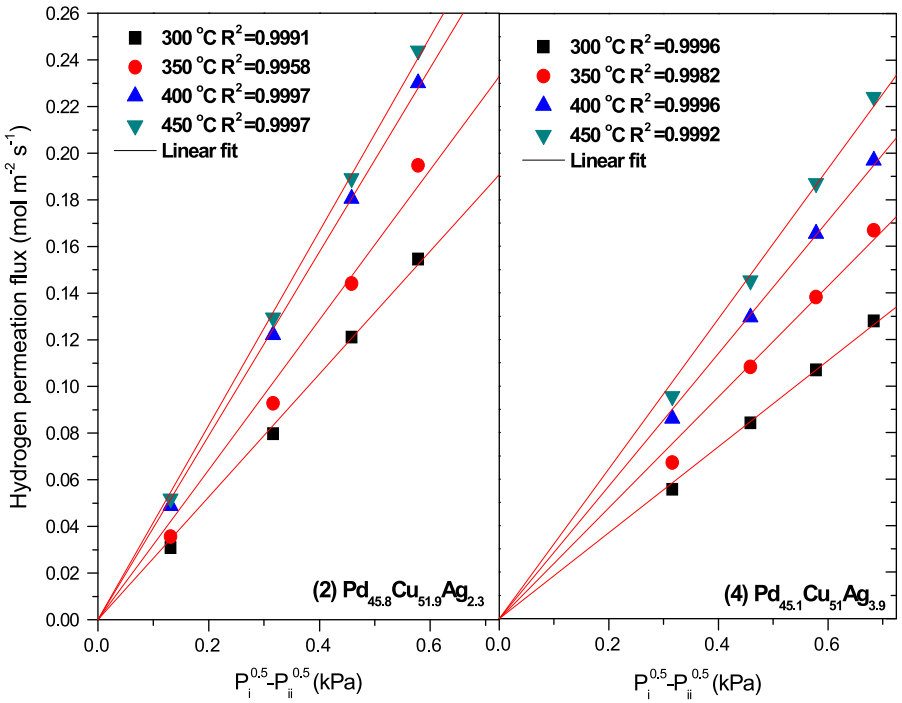

Fig. 7. Hydrogen permeation flux at several temperatures as a function of hydrogen differential pressures: (a) $Pd_{45.8}Cu_{51.9}Ag_{2.3}$ (sample 3), and (b) $Pd_{45.1}Cu_{51}Ag_{3.9}$ (sample 4).

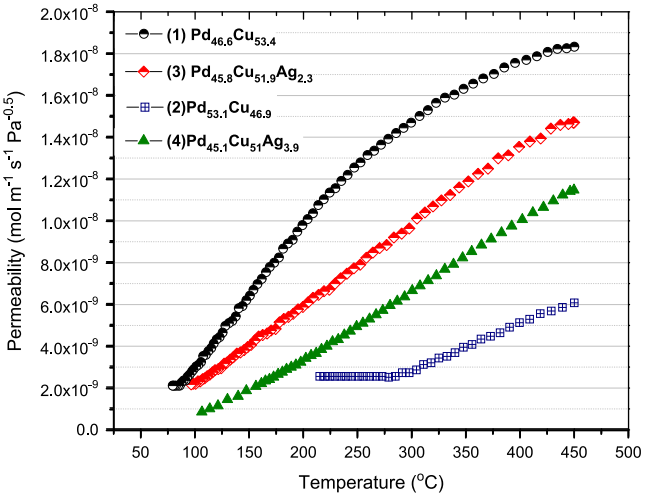

Fig. 8. 2nd cycle heating hydrogen permeability profiles as a function of temperature, of $Pd_{46.6}Cu_{53.4}$ (sample 1), $Pd_{45.8}Cu_{51.9}Ag_{2.3}$ (sample 3), $Pd_{53.1}Cu_{46.9}$ (sample 2), and $Pd_{45.1}Cu_{51}Ag_{3.9}$ (sample 4). Continuous hydrogen flow of 445 kPa was supplied on the upstream side of the vessel whilst the downstream side was kept at static hydrogen pressure of 100 kPa during measurements. A heating rate of 2 °C min^{-1} was applied.

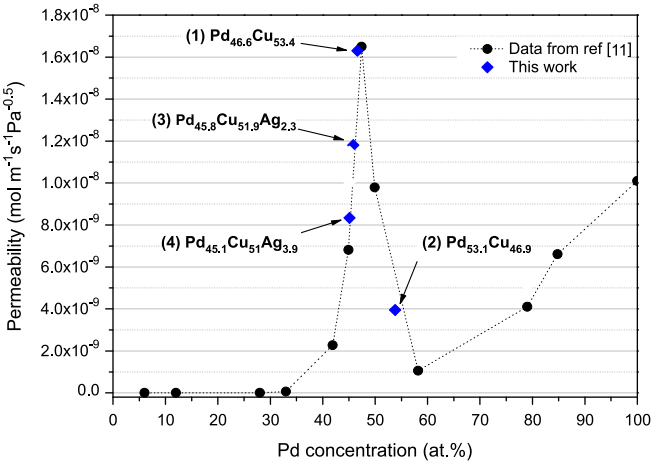

Fig. 9. Hydrogen permeability values of the Pd–Cu binary alloys as a function of Pd concentration at 350 °C. Included are the hydrogen permeability values of the binary and ternary samples in this study at 350 °C for comparison. Dotted line is a guide for the eye.

Accordingly, it is expected that sample (3) shows a lower hydrogen permeability than its binary alloy at higher temperatures than 350 °C, due to the reduced diffusion coefficient as a result of Ag addition (Fig. 6a). Hence, it is suggested that adding a small amount of Ag to the bcc Pd–Cu alloys may reduce the permeability as a result of a lower diffusion coefficient particularly at higher temperatures than 350 °C.

A direct comparison of sample (4) with the corresponding binary alloy may not be appropriate as XRD spectra showed the sample is not single bcc phase. However, if a comparison is made with sample (2), with the mixed (bcc+fcc) structure, the higher permeability of sample (4) at 350 °C may be explained by the improved hydrogen solubility observed in this sample. It was shown in Fig. 6c and d that sample (4) has lower hydrogen diffusion coefficients but higher solubility values than that of sample (2) within the studied temperature range. Lower hydrogen diffusivity values of sample (4) in comparison with sample (2) can be attributed to both its higher Cu concentration [42] and Ag addition [33]. However, the improved hydrogen solubility values should be related to the Ag addition [33] as an increase in the Cu concentration is expected to reduce the hydrogen solubility in Pd–Cu alloys [43,44]. In addition, as shown in Fig. 2g and h, the relative amount of fcc phase is lower in sample (4) than in sample (2), after annealing at 400 °C. This confirms the general findings of earlier works [33], which has shown the effectiveness of Ag addition in improving hydrogen solubility in the fcc phase and increasing the overall hydrogen permeability.

Therefore, unlike the ternary alloy with a bcc structure (sample 3), where hydrogen diffusion appears to be dominant in controlling permeability, solubility of hydrogen is proposed to have a substantial effect on the hydrogen permeability of the ternary alloy with a mixed structure (sample 4). Accordingly, the higher permeability values that are observed for sample (4) in comparison with sample (2) at higher

temperatures than 350 °C in Fig. 8 are suggested to be the result of higher hydrogen solubility values for sample (4).

4. Discussion

The experimental results for the binary Pd–Cu and ternary Pd–Cu–Ag alloys in this study show the interaction between crystal structure, diffusion and solubility in determining hydrogen permeability. Several theoretical studies have considered the mechanisms underlying hydrogen diffusion and solubility in fcc and bcc Pd–Cu binary and ternary alloys [31–33,38].

In the disordered fcc Pd–Cu alloys interstitial H atoms can reside in either Octahedral (O site), or Tetrahedral sites (T site). Hydrogen in the ordered bcc Pd–Cu prefers to bind near tetrahedral site positions. Long range hydrogen diffusion in both fcc and bcc lattice at elevated temperatures takes place by a series of hops between these interstitial sites. Each hop has to overcome the energy barriers between interstitial sites, known as the Transition State (TS) [32,38]. Two hydrogen diffusion pathways were suggested for the bcc Pd–Cu alloy based on the interstitial hydrogen jumps through the Cu_2Pd and Pd_2Cu based triangular faces in T sites. However, hydrogen diffusion through the Cu_2Pd triangular face was proposed to be the dominant path because of the lower activation energy, *i.e.* the required energy to bypass the TS between the two T sites [38]. In addition DFT calculations for hydrogen diffusion in the Pd–Cu–Ag fcc phase showed that the presence of Ag in the window forming TS leads to a significant increase in its energy. Therefore, hopping through TS with one or more Ag atoms is less favourable [33]. Hence, it is possible that such a phenomenon may also occur for the Pd–Cu bcc phase when small concentrations of Ag are present. The lower diffusion coefficients of sample (3) at temperatures higher than 350 °C, in comparison with sample (1) (Fig. 6a), may be related to the Ag substitution for Pd or Cu in the Cu_2Pd triangular face and an increase in the hydrogen diffusion activation energy. Activation energies of 5.8 and 10.2 kJ $mol^{-1}H_2$ (350–400 °C) were obtained for hydrogen permeation in samples (1) and (3), respectively. It is well known that the activation energy required for hydrogen permeation is defined by the sum of the activation energies required for the hydrogen diffusion and solubility (heat of solution) [14]. It was shown that hydrogen solubility of sample (3) is much higher than sample (1) (Fig. 6b), which suggests a reduction in the heat of solution in sample (3). This further confirms that hydrogen solubility has a relatively small effect on the hydrogen permeability in the bcc phase and it is mainly dominated by hydrogen diffusion.

In addition, for the Pd–Cu–Ag ternary alloys with an fcc structure, it was shown [33] that increasing the Ag content raises the diffusion activation energy barrier which is defined as the required energy for hydrogen hopping from an O site to the nearest T site passing a TS. Also, the possibility of direct hopping from an O site to O site was put forward for Pd–Ag, Pd–Cu–Ag and Pd–Cu–Au alloys, where additional atoms are much larger than host metal in an alloy [45]. In such a situation, a T site is not a local minimum in energy and hydrogen atoms should move via the next available O site passing a TS with higher energy barrier. Accordingly, lower diffusion coefficients of sample (4) in comparison with sample (2) observed in this study, may be also related to the less favourable hopping through TS with one or more Ag atoms and an increase in the activation energy either for hopping from O site to the nearest T site or O site to the nearest O site. Activation energies of 17.6 and 13.3 kJ $mol^{-1}H_2$ (350–400 °C) were obtained for hydrogen permeation in samples (2) and (4), respectively. Although, the activation energy for the hydrogen diffusion seems to be higher in sample (4) due to the lower diffusion coefficients (Fig. 6c), its overall activation energy is still lower than sample (2). This denotes a significant contribution from the heat of solution (Fig. 6d) on the overall observed activation energy. Therefore, in contrast to the marked effects of Ag alloying on hydrogen diffusion in the bcc phase, our results show that the effect of Ag on hydrogen diffusion for the fcc phase is not significant and has a relatively small effect on the hydrogen permeability.

It should be noted that solution of hydrogen into a metal is an endothermic process. However, the solubility of hydrogen in a metal can either increase or decrease with increasing temperature, depending on the balance between the tendency of a metal to only form a simple solution of hydrogen (endothermic) or by the formation of pseudo-metallic ordered hydride phases (exothermic) [46,47]. The tendency of palladium to form ordered hydride phases is well known, which results in the hydrogen embrittlement problem [2]. Alloying Pd with more than 30 at% Cu has been shown to effectively supress the formation of pseudo-metallic ordered hydride phases at room temperature [43]. Therefore, regardless of the bcc or fcc structure of the samples in this study, formation of a simple solid solution implies to the identical hydrogen–metal interactions. Hence, reductions in the heat of solutions should be related to the effect of Ag addition.

In general, hydrogen solubility in Pd-alloys is influenced by the lattice expansion or contraction relative to pure Pd [30,33]. For instance, higher hydrogen solubility values are observed for isoelectronic Pd–Y_8 alloy than Pd–Ag_{24}, where the nominal size factor with respect to Pd in the case of each alloy is 29% and 5%, respectively [35]. It might be assumed that as Ag has a larger atomic size than Pd and Cu, substitution of Ag for these elements in Pd–Cu alloy should result in lattice expansion of the alloy, hence higher hydrogen solubility. Furthermore, theoretical calculations for fcc Pd–Cu–Ag alloys showed that once a small amount of Ag is substituted for Pd, hydrogen solubility is improved as a result of lattice expansion which favours the hydrogen binding energy in O sites [33]. However, it was also noted [33] that hydrogen solubility cannot be adequately explained only based on the lattice expansion. This is also reflected in our results where sample (4) with smaller lattice constant (Table 1) shows higher hydrogen solubility than that of sample (2). Another factor which needs to be considered is the availability of free atomic sites for hydrogen occupation. Once the Ag content is increased, the binding energies of hydrogen in O sites become less favourable. This is because of the existence of more Ag atoms in the Nearest Neighbour (NN) shell of the interstitial site that limits the available free space for hydrogen occupation [10,33]. In addition, hydrogen solubility in the fcc binary and ternary Pd-alloys may be influenced by the chemical potential of alloys-H system, which itself is a function of ionic diameter and hydrogen–solute metal pair interaction free energy. Using this approach, it was shown [48] that the higher chemical interaction between the solute metal and hydrogen can encourage solubility in the alloy.

Whilst relative atomic size is influential in determining hydrogen solubility, there are electronic effects associated with substitutional atoms, which also contributes to hydrogen solubility in the Pd alloys. It was shown [49–51] that whilst additional lattice expansion based on the filling of the Pd 4d electron states by the solute valence electrons can be achieved, hydrogen solubility decreases as more Pd 4d-bands are occupied. Thus, the electronic effect of a given substitutional element is defined by its valence electron [48]. Whilst, the electronic effect may be dominated by the valence electrons, small variation in the charge density of the alloying species may affect the stability of the hydrogen in various interstitial sites. The strength of the binding will be related to the electronegativity of the substitutional atom and generally the binding stability would be reduced when hydrogen gains less charge [52]. Although Ag has the same number of valence electrons as Cu, their electronic orbitals are spatially different

due to the size and electronegativity difference. Exact comparisons of the effects of the spatial electronic configurations of Cu and Ag in the Pd–Cu–Ag alloys would require detailed evaluation of the density of states at specific crystallographic sites, which is beyond the scope of the present work. Nevertheless, the electronic effect seems to be more pronounced in the alloys with a high Pd content.

Hence, hydrogen solubility in the Pd–Cu–Ag fcc phase seems to be determined by a combination of effects: lattice expansion, availability of free atomic sites for hydrogen occupation (geometrical), solute metal–hydrogen interaction (chemical effect), and electronic structure. The higher hydrogen solubility values observed in this study for the ternary alloys (Fig. 6) are therefore mainly attributed to the replacement of Ag for Pd and Cu leading to a lattice expansion and a more favourable Ag–H chemical effect [48]. However, due to the low concentration of Ag in the Pd–Cu–Ag alloys used here, the effect of the reduction in the available free atomic sites for hydrogen solubility may not be substantial. Furthermore, according to our results, whilst Ag addition leads to an enhancement in the hydrogen solubility in the $Pd_{45.8}Cu_{51.9}Ag_{2.3}$ bcc phase, overall it leads to the permeability to be relatively unchanged. However, an increase in the hydrogen solubility appears to have a significant effect for hydrogen permeability in the fcc phase. These effects could be further investigated in fcc Pd–Cu binary alloys by adding a small amount of selective elements with high hydrogen affinity, thus satisfying the requirement reported here for the improvement of hydrogen solubility. In addition, further investigation is required in varying the amount of Ag addition to the bcc phase of Pd–Cu alloy, to try to establish its effect on the formation of fcc phase under a range of hydrogen atmospheres. Tuning Ag concentration in the bcc phase of the Pd–Cu alloy may offer a new series of hydrogen separation membranes having acceptable hydrogen permeability with a degree of tolerance to surface poisoning.

5. Conclusions

The effects of small (2.3 and 3.9 at%) Ag additions on the structure and hydrogen permeation behaviour of Pd–Cu alloys in the bcc region of the phase diagram, were investigated. Structural analysis by XRD indicated a lattice expansion as a result of Ag addition. Furthermore, whilst the bcc structure was retained during heating of the $Pd_{45.8}Cu_{51.9}Ag_{2.3}$ ternary alloy up to 600 °C, formation of the fcc phase was promoted at higher temperatures in the $Pd_{45.1}Cu_{51}Ag_{3.9}$ ternary alloy. It was observed that in both Pd–Cu–Ag alloys with bcc and (bcc+fcc) phases, Ag always lowers the diffusion coefficients of hydrogen in the Pd–Cu–Ag alloys compared to the binary Pd–Cu alloys. This is probably due to an increase in the diffusion activation barrier and less favourable diffusion through the transition state containing Ag atoms. In contrast, the hydrogen solubilities of the ternary Pd–Cu–Ag alloys studied here were always higher than those of the binary Pd–Cu alloys, probably as a result of the lattice expansion and high Ag–H affinity. The hydrogen permeability of the $Pd_{45.8}Cu_{51.9}Ag_{2.3}$ and $Pd_{46.6}Cu_{53.4}$ alloys with bcc structure suggested that an enhancement in the hydrogen solubility of the $Pd_{45.8}Cu_{51.9}Ag_{2.3}$ sample has a relatively small effect on the permeability because the hydrogen permeability in the bcc phase is mainly dominated by hydrogen diffusion. The situation is reversed in the fcc phase, where it is the variation in the hydrogen solubility which has a substantial effect on the permeability. Therefore, higher hydrogen permeability can be achieved, through an enhancement of the hydrogen solubility of Pd–Cu alloys containing the fcc phase.

Acknowledgements

The authors are grateful to Johnson Matthey Noble Metals (Royston, UK) for the provision of rolled Pd alloy samples. Support from the EPSRC SUPERGEN Delivery of Sustainable Hydrogen (EP/G01244X/1) and the Birmingham Science City Hydrogen Energy projects, is gratefully acknowledged.

References

[1] G. Alefeld, J. Völkl (Eds.), Hydrogen in Metals II: Application-Oriented Properties, Springer-Verlag, Berlin, 1978.
[2] A.G. Knapton, Palladium alloys for hydrogen diffusion membranes, Platinum Metals Review 21 (2) (1977) 44.
[3] B.D. Morreale, B.H. Howard, O. Iyoha, R.M. Enick, C. Ling, D.S. Sholl, Experimental and computational prediction of the hydrogen transport properties of Pd_4S, Industrial and Engineering Chemistry Research 46 (19) (2007) 6313.
[4] E. Ozdogan, J. Wilcox, Investigation of H_2 and H_2S adsorption on niobium- and copper doped palladium surfaces, Journal of Physical Chemistry B 114 (2010) 12851.
[5] G.J. Grashoff, C.E. Pilkington, C.W. Corti, The purification of hydrogen: a review of the technology emphasizing the current status of palladium membrane diffusion, Platinum Metals Review 27 (4) (1983) 157.
[6] S. Adhikari, S. Fernando, Hydrogen membrane separation techniques, Industrial and Engineering Chemistry Research 45 (2006) 875.
[7] A. Basile, F. Gallucci, S. Tosti, Synthesis, characterisation, and application of palladium membranes, Membrane Science and Technology 13 (2008) 255.
[8] S.N. Paglieri, J.D. Way, Innovation in palladium membrane research, Separation and Purification Method 31 (1) (2002) 1.
[9] C.G. Sonwane, J. Wilcox, Y.H. Ma, Achieving optimum hydrogen permeability in PdAg and PdAu alloys, Journal of Chemical Physics 125 (2006) 184714.
[10] C.G. Sonwane, J. Wilcox, Y.H. Ma, Solubility of hydrogen in PdAg and PdAu binary alloys using density functional theory, Journal of Physical Chemistry B 110 (2006) 24549.
[11] D.L. McKinley, Methods for hydrogen separation and purification. US Patent 3,439,474, 1969.
[12] J. Piper, Diffusion of hydrogen in copper–palladium alloys, Journal of Applied Physics 37 (2) (1966) 715.
[13] F. Roa, M.J. Block, J.D. Way, The influence of alloy composition on the H_2 flux of composite Pd–Cu membranes, Desalination 147 (2002) 411.
[14] L. Yuan, A. Goldbach, H. Xu, Segregation and H_2 transport rate control in body-centered cubic PdCu membranes, Journal of Physical Chemistry B 111 (2007) 10952.
[15] L. Yuan, A. Goldbach, H. Xu, Real-time monitoring of metal deposition and segregation phenomena during preparation of PdCu membranes, Journal of Membrane Science 322 (2008) 39.
[16] L. Yuan, A. Goldbach, H. Xu, Permeation hysteresis in PdCu membranes, Journal of Physical Chemistry B 112 (2008) 12692.
[17] S.M. Opalka, W. Huang, D. Wang, T.B. Flanagan, O.M. LØvvik, S.C. Emerson, Y. She, T.H. Vanderspurt, Hydrogen interaction with the PdCu ordered B2 alloy, Journal of Alloys and Compounds 446–447 (2007) 583.
[18] A. Goldbach, L. Yuan, H. Xu, Impact of the fcc/bcc phase transition on the homogeneity and behavior of PdCu membranes, Separation and Purification Technology 73 (2010) 65.
[19] P.R. Subramanian, D.E. Laughlin, Cu–Pd (copper–palladium), Journal of Phase Equilibria 12 (2) (1991) 231.
[20] W. Huang, S.M. Opalka, D. Wang, T.B. Flangan, Thermodynamic modeling of the Cu–Pd–H system, Computer Coupling of Phase Diagrams and Thermochemistry (2007)315.
[21] M. Li, Z. Du, C. Guo, C. Li, A thermodynamic modeling of the Cu–Pd system, Computer Coupling of Phase Diagrams and Thermochemistry 32 (2008) 439.
[22] J.R. Warren, The effect of hydrogen on palladium–copper based membranes for hydrogen purification (M.Sc. thesis), University of Birmingham, 2010.
[23] T.A. Peters, T. Kaleta, M. Stange, R. Bredesen, Hydrogen transport through a selection of thin Pd-alloy membranes: membrane stability, H_2S inhibition, and flux recovery in hydrogen and simulated WGS mixtures, Catalysis Today 193 (2012) 8.
[24] C.P. O'Brien, B.H. Howard, J.B. Miller, B.D. Morreale, A.J. Gellman, Inhibition of hydrogen transport through Pd and Pd47Cu53 membranes by H_2S at 350 °C, Journal of Membrane Science 349 (2010) 380.
[25] B.D. Morreale, M.V. Ciocco, B.H. Howard, R.P. Killmeyer, A.V. Cugini, R.M. Enick, Effect of hydrogen-sulfide on the hydrogen permeance of palladium–copper alloys at elevated temperatures, Journal of Membrane Science 241 (2004) 219.
[26] P. Kamakoti, B.D. Morreale, M.V. Coicco, B.H. Howard, R.P. Killmeyer, A.V. Cugini, D.S. Sholl, Prediction of hydrogen flux through sulfur-tolerant binary alloy membranes, Science 307 (2005) 569.
[27] S.M. Opalka, O.M. LØvvik, S.C. Emerson, Y. She, T.H. Vanderspurt, Electronic origins for sulfur interactions with palladium alloys for hydrogen-selective membranes, Journal of Membrane Science 375 (2011) 96.
[28] A.M. Tarditi, F. Braun, L.M. Cornaglia, Novel PdAgCu ternary alloys: hydrogen permeation and surface properties, Applied Surface Science 257 (2011) 6626.
[29] A.M. Tarditi, L.M. Cornaglia, Novel PdAgCu ternary alloys as promising materials for hydrogen separation membranes: synthesis and characterisation, Surface Science 605 (2011) 62.
[30] T.A. Peters, T. Kaleta, M. Stange, R. Bredesen, Development of thin binary and ternary Pd-based alloys membranes for use in hydrogen production, Journal of Membrane Science 383 (2011) 124.

[31] P. Kamakoti, D.S. Sholl, Towards first principles-based identification of ternary alloys for hydrogen purification methods, Journal of Membrane Science 279 (2006) 94.
[32] L. Semidey-Flecha, C. Ling, D.S. Sholl, Detailed first principles models of hydrogen permeation through PdCu-based ternary alloys, Journal of Membrane Science (2010) 384.
[33] C. Ling, L. Semidey-Flecha, D.S. Sholl, First principles screening of PdCuAg ternary alloys as H_2 purification membranes, Journal of Membrane Science 371 (2011) 189.
[34] Sean Fletcher, Thin-film palladium–yttrium membranes for hydrogen separation (Ph.D. thesis), University of Birmingham, 2009.
[35] D.T. Hughes, I.R. Harris, A comparative study of hydrogen permeabilities and solubilities in some palladium solid solution alloys, Journal of Less Common Metals 61 (1978) P9.
[36] D. Fisher, D.M. Chisdes, T.B. Flanagan, Solution of hydrogen in palladium/copper alloys, Journal of Solid State Chemistry 20 (1977) 149.
[37] R. Burch, R.G. Buss, Absorption of hydrogen by palladium–copper alloys, Journal of Chemical Society, Faraday Transactions 1 (71) (1975) 913.
[38] P. Kamakoti, D.S. Sholl, A comparison of hydrogen diffusivities in Pd and CuPd alloys using density functional theory, Journal of Membrane Science 225 (2003) 145.
[39] G. Alefeld, J. VÖlkl (Eds.), Hydrogen in Metals I: Application-Oriented Properties, Springer-Verlag, Berlin, 1978.
[40] C. Decaux, R. Ngameni, D. Solas, S. Grigoriev, P. Millet, Time and frequency domain analysis of hydrogen permeation across PdCu metallic membranes for hydrogen purification, International Journal of Hydrogen Energy 35 (2010) 4883.
[41] S. Yun, S.T. Oyama, Correlation in palladium membranes for hydrogen separation: a review, Journal of Membrane Science 375 (2011) 28.
[42] P. Kamakoti, D.S. Sholl, Ab initio lattice gas modelling of interstitial hydrogen diffusion in CuPd alloys, Physical Review B 71 (2005) 014301.
[43] R. Burch, R.G. Buss, Absorption of hydrogen by palladium–copper alloys, Journal of the Chemical Society, Farday Transactions 71 (1) (1975) 913.
[44] T.B. Flanagan, D.M. Chisdes, Solubility of hydrogen (1 atm, 298 K) in some copper/palladium alloys, Solid State Communications 16 (1975) 529.
[45] L. Semidey-Flecha, D.S. Sholl, Combining density functional theory and cluster expansion methods to predict H_2 permeance through Pd-based binary alloy membranes, Journal of Chemical Physics 128 (2008) 144701.
[46] M.D. Dolan, Non-Pd bcc membranes for industrial hydrogen separation, Journal of Membrane Science 362 (2010) 12.
[47] P. Cotterill, The hydrogen embrittlement of metals, Progress in Materials Science 9 (1961) 205.
[48] S. Ramaprabhu, Thermodynamics and stability of dissolved hydrogenation in Pd rich binary $Pd_{1-x}Z_x$ and ternary $Pd_{1-x}Z_xZ'_y$ solid solution alloys, International Journal of Hydrogen Energy 23 (9) (1998) 787.
[49] I.R. Harris, M. Norman, Observation on the lattice spacing of some α Pd–X solid solutions and some Pd_3X phases, Journal of the Less Common Metals 22 (1970) 127.
[50] D. Fort, J.P.G. Farr, I.R. Harris, A comparison of palladium–silver and palladium–yttrium alloys as hydrogen separation membranes, Journal of the Less Common Metals 39 (1975) 293.
[51] M.L. Doyle, I.R. Harris, Palladium-rare earth alloys: their order–disorder transformations and behaviour with hydrogen, Platinum Metals Review 32 (3) (1988) 130.
[52] S. Aboud, J. Wilcox, A density functional study of the charge state of hydrogen in metal hydrides, Journal of Physical Chemistry C 114 (2010) 10978.